



Cite this: *Phys. Chem. Chem. Phys.*,  
2016, 18, 10781

# Methanol synthesis *via* CO<sub>2</sub> hydrogenation over a Au/ZnO catalyst: an isotope labelling study on the role of CO in the reaction process†

Yeusy Hartadi, Daniel Widmann and R. Jürgen Behm\*

Methanol synthesis for chemical energy storage, *via* hydrogenation of CO<sub>2</sub> with H<sub>2</sub> produced by renewable energies, is usually accompanied by the undesired formation of CO *via* the reverse water–gas shift reaction. Aiming at a better mechanistic understanding of methanol formation from CO<sub>2</sub>/H<sub>2</sub> on highly selective supported Au/ZnO catalysts we have investigated the role of CO in the reaction process using isotope labelling experiments. Using <sup>13</sup>C-labelled CO<sub>2</sub>, we found for reaction at 5 bar and 240 °C that (i) the methanol formation rate is significantly higher in CO<sub>2</sub>-containing gas mixtures than in a CO<sub>2</sub>-free mixture and (ii) in mixtures containing both CO<sub>2</sub> and CO methanol formation from CO increases with the CO content up to 1% CO, and then remains at 20% of the total methanol formation up to a CO<sub>2</sub>/CO ratio of 1/1, making CO<sub>2</sub> the preferred carbon source in these mixtures. A shift in the preferred carbon source for MeOH from CO<sub>2</sub> towards CO is observed with increasing reaction temperatures between 240 °C and 300 °C. At even higher temperatures CO is expected to become the dominant carbon source. The consequences of these findings for the application of Au/ZnO catalysts for chemical storage of renewable energies are discussed.

Received 10th November 2015,  
Accepted 15th February 2016

DOI: 10.1039/c5cp06888f

www.rsc.org/pccp

## 1. Introduction

A promising approach in renewable energy concepts to overcome natural fluctuations in the supply of renewable energy involves the conversion and storage of excess electrical energy in the form of chemical energy.<sup>1,2</sup> Methanol (MeOH) as a storage molecule is of particular interest, since it can be easily stored and transported.<sup>3,4</sup> It can be used as a source of CO<sub>2</sub>-neutral synthetic fuels<sup>5</sup> or as feedstock for synthesis of a variety of basic materials.<sup>4,6</sup> At present MeOH is mainly produced from syngas containing CO, CO<sub>2</sub> and H<sub>2</sub>, which is obtained from catalytic reforming of fossil fuels.<sup>6</sup> However, by replacing fossil fuels as the carbon source with anthropogenic CO<sub>2</sub> from industrial exhaust or coal power plants,<sup>7–11</sup> for example, so-called “green MeOH” can be produced.<sup>12–17</sup> This way also the overall CO<sub>2</sub> emission can be diminished.<sup>7–17</sup> Technically this process was applied first in the ‘Emission-to-Liquid’ (ETL) technology developed by Carbon Recycling International (CRI), which since 2011 has been operating the commercial George Olah Renewable Methanol Plant with a production capacity of 5 million liters per year.<sup>13,18</sup>

In the industrial MeOH production from CO<sub>2</sub>-enriched syngas typically Cu/ZnO + MeO<sub>x</sub> catalysts are employed.<sup>6</sup> These have been

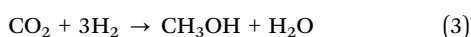
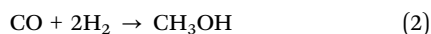
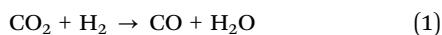
optimized to a very high performance level under industrial relevant reaction conditions (at elevated temperatures and pressures) because of the enormous importance of industrial MeOH production.<sup>19–28</sup> Accordingly, one may assume that it is also a reasonable, highly active candidate for CO<sub>2</sub> hydrogenation for the above described application. MeOH formation from CO<sub>2</sub>, however, is usually accompanied by the undesirable formation of CO *via* the reverse water-gas shift (RWGS) reaction.<sup>16,29–33</sup> Thus, besides high MeOH formation rates, the selectivity towards MeOH formation represents another crucial factor that has to be considered. So far only a very limited number of catalytic systems is known, which show no or almost no activity for the CO formation in CO<sub>2</sub>/H<sub>2</sub> reaction gas mixtures for MeOH formation, for example, differently promoted Cu-based catalysts,<sup>34–36</sup> Au and Ag supported on 3ZnO-ZrO<sub>2</sub>,<sup>35</sup> carbon nanotubes supported Pd-ZnO catalysts,<sup>37</sup> or a pre-reduced LaCr<sub>0.5</sub>Cu<sub>0.5</sub>O<sub>3</sub> catalyst.<sup>38</sup> Previous studies on commercial Cu-based catalysts have shown that these are active for the reverse water-gas shift (RWGS) reaction between 230 and 260 °C, resulting in the formation of rather large amounts of CO in addition to MeOH and, hence, rather low selectivities towards MeOH.<sup>31,32,39–42</sup> For example, testing the activity and selectivity of two commercial Cu/ZnO/Al<sub>2</sub>O<sub>3</sub> catalyst samples at total pressures between 5 and 50 bar (CO<sub>2</sub>/H<sub>2</sub> = 1/3), we recently obtained selectivities towards MeOH of only 16% and 42%, respectively.<sup>31</sup> Some supported Au catalysts, on the other hand, are significantly more selective compared to the

*Institute of Surface Chemistry and Catalysis, Ulm University,  
Albert-Einstein-Allee 47, D-89081 Ulm, Germany. E-mail: juergen.behm@uni-ulm.de*  
† Electronic supplementary information (ESI) available. See DOI: 10.1039/c5cp06888f



commercial Cu-based catalysts under identical reaction conditions.<sup>31,32</sup> This is particularly true for Au/ZnO.<sup>31,32</sup> While their noble metal mass-normalized activity for MeOH is comparable to that of Cu catalysts, their selectivity is much higher, about 50% at 5 bar and almost 70% at 50 bar.<sup>31,32</sup> A more detailed comparison of the catalytic performance (activities and selectivities) over commercial Cu- and Au-based catalysts is given in ref. 31 and 32. At present, the much higher price of gold compared to that of Cu renders CO<sub>2</sub> hydrogenation to MeOH on supported Au catalysts economically not competitive, but these previous findings clearly demonstrated their promising potential for certain applications, *e.g.*, for small scale operation under dynamic operation conditions, as expected in renewable energy concepts.<sup>31</sup> They are also very interesting from a scientific point of view, to understand the origin of the high activity and selectivity of Au/ZnO catalysts for CO<sub>2</sub> hydrogenation to MeOH. Here it is worth mentioning that for both Au- and Cu-based catalysts the presence of Zn species seems to be mandatory in order to achieve high MeOH formation rates as well as selectivities.<sup>15,31,43</sup> This suggests that Au/ZnO and Cu/ZnO benefit from the same effect, namely the partial reduction of ZnO under reaction conditions in the highly reductive atmosphere and subsequent migration of ZnO<sub>x</sub> surface species on the Au or Cu nanoparticles, resulting either in the formation of a AuZn or CuZn (surface) alloy, or the formation of a ZnO<sub>x</sub> shell.<sup>15,43–47</sup> While for Cu-based catalysts the formation of such species and their contribution in the reaction mechanism of CO hydrogenation and CO<sub>2</sub> hydrogenation to MeOH was already demonstrated,<sup>15,43–47</sup> similar information on Au/ZnO catalysts is scarce so far.<sup>31</sup> Nevertheless, it may be envisioned that such effects are also present on Au surfaces, which can thus explain the superior catalytic performance of Au/ZnO for the MeOH formation from CO<sub>2</sub> and H<sub>2</sub> as compared to other metal oxide supported Au catalysts.<sup>31</sup> Interestingly, Martin *et al.* just recently demonstrated the promotion of Cu–ZnO–Al<sub>2</sub>O<sub>3</sub> catalysts for the MeOH formation by addition of gold, which they explained by a stabilization of metallic Cu<sup>0</sup> species in close vicinity to ZnO.<sup>36</sup>

Although Au/ZnO catalysts predominantly produce MeOH, there will always be significant amounts of CO present in the reaction atmosphere because of its formation *via* the reverse water-gas shift reaction. In particular this is the case at the end of the catalyst bed in practical applications, which aim at high CO<sub>2</sub> conversions. Hence, there will be an increasing CO partial pressure along the catalyst bed. In order to minimize any detrimental effects of CO on the main reaction, a detailed understanding of its influence is essential. Recently we reported on the influence of CO on the MeOH formation characteristics in the presence of low and high CO partial pressures. Based on the significantly higher activities for MeOH formation from pure CO<sub>2</sub>/H<sub>2</sub> mixtures than obtained upon addition of CO to the reaction gas feed, we proposed that CO<sub>2</sub> is not converted to CO first, *via* the RWGS reaction (eqn (1)), which is subsequently hydrogenated to MeOH (eqn (2)), but is directly hydrogenated to MeOH (eqn (3)).<sup>32</sup>



In that case CO does not represent a reaction intermediate in the CO<sub>2</sub> hydrogenation, but a byproduct in the direct hydrogenation of CO<sub>2</sub>, and both, CO<sub>2</sub> hydrogenation and CO hydrogenation, proceed parallel to each other under the reaction conditions used in that study. Furthermore, it seems likely that CO<sub>2</sub> is the main carbon source for MeOH in CO<sub>2</sub>/CO/H<sub>2</sub> mixtures. A definite proof for this proposal, however, was not possible in that study, since the individual contributions of CO and CO<sub>2</sub> to the MeOH formation from a CO<sub>2</sub>/CO/H<sub>2</sub> mixture could not be determined.

This is the topic of the present study, in which we explored the activities of a Au/ZnO catalyst for CO and CO<sub>2</sub> hydrogenation in a gas mixture containing both components, CO<sub>2</sub> and CO, together with H<sub>2</sub> by isotope labelling techniques. By adding well-defined amounts of <sup>12</sup>CO (between 0.5 and 15%) to a reaction gas mixture containing 15% <sup>13</sup>CO<sub>2</sub> (CO<sub>2</sub>/H<sub>2</sub> = 1/3) and following the corresponding changes in the amounts of <sup>13</sup>CH<sub>3</sub>OH and <sup>12</sup>CH<sub>3</sub>OH formation, we could quantify the individual contributions of <sup>13</sup>CO<sub>2</sub> and <sup>12</sup>CO to the total amount of MeOH formed. Besides, one can also derive insights into the reaction pathway for CO<sub>2</sub> and CO hydrogenation from such studies, in particular whether CO<sub>2</sub> is directly hydrogenated to MeOH or whether it is first converted to CO, which is subsequently hydrogenated.

In contrast to Cu-based catalysts, where a number of previous studies presented ample evidence that the main carbon source for MeOH from synthesis gas containing both CO<sub>2</sub> and CO is CO<sub>2</sub>, *e.g.*, by kinetic investigations,<sup>48,49</sup> isotope labelling measurements<sup>45,48,50–52</sup> and theoretical calculations,<sup>29</sup> direct information to resolve this question for Au catalysts is not yet available.

In the following, we will, after a short summary of the physical properties of the commercial Au/ZnO catalyst used in this study (Section 3.1), present the results of the kinetic isotope labelling measurements using <sup>13</sup>C labelled CO<sub>2</sub> and <sup>12</sup>CO (Section 3.2). The influence of the reaction temperature, upon increasing it from 240 °C to 300 °C for a fixed ratio of <sup>13</sup>CO<sub>2</sub>/<sup>12</sup>CO, is elucidated and discussed in Section 3.3. In addition to mechanistic insights we finally discuss the consequences of these findings for potential applications of Au/ZnO catalysts for the chemical storage of renewable energies.

## 2. Experimental

### 2.1. Preparation and characterization of Au/ZnO

For all measurements we used a commercially available Au/ZnO catalyst prepared by deposition precipitation (DP) from STREM Chemicals. Prior to the kinetic measurements, the catalyst was calcined *in situ* in a flow of 20 Nml min<sup>−1</sup> of 1% O<sub>2</sub> in Ar at 400 °C and atmospheric pressure for 1 h (denoted O400). Subsequently, the catalyst was cooled to the reaction temperature (240 °C) in a flow of Ar. The Au loading, the Au particle size and the surface area of the Au/ZnO catalyst after O400 were measured by inductively coupled plasma optical emission spectroscopy (ICP-OES, Horiba Jovin Yvon Ultima 2), transmission electron microscopy



(TEM, JEOL 1400) and low temperature N<sub>2</sub> adsorption (BET, Quantachrome Quadrasorb SI), respectively. Based on the Au particle size distribution obtained from the TEM images, the volume–area mean diameter as well as the Au dispersion were calculated. For calculation of the latter we assumed hemispherical Au nanoparticles with  $1.15 \times 10^{15} \text{ cm}^{-2}$  Au surface atoms.

## 2.2. Kinetic measurements

Kinetic measurements were performed at 5 bar total pressure and at a reaction temperature of 240 °C under differential reaction conditions in a glass-lined stainless steel tube micro reactor (inner diameter 4 mm). The lower pressure of 5 bar compared to previous kinetic measurements at 50 bar<sup>32</sup> was chosen to keep the consumption of expensive <sup>13</sup>CO<sub>2</sub> at a tolerable level. Note that the total conversions of CO<sub>2</sub> and CO (1% at the most in all kinetic experiments) were significantly below the maximum conversion given by the thermodynamic equilibrium, which is at approximately 15% and 8% for CO<sub>2</sub> (to both MeOH and CO) and CO (to MeOH) hydrogenation, respectively, under present reaction conditions. For all measurements we used about 200 mg of pure Au/ZnO catalyst powder, which was fixed in the center of the micro reactor using quartz wool plugs on either side. This results in a catalyst bed length of about 2 cm. High purity reaction gases were supplied by Westfalen (H<sub>2</sub> 5.0, Ar 5.0 and CO 4.7) and Campro Scientific (<sup>13</sup>CO<sub>2</sub>, 99 atom% <sup>13</sup>C). The gases were mixed by mass flow controllers (Brooks Instrument SLA5850) in order to realize the desired reaction gas composition. A backpressure controller (Tescom ER5000) was used in order to regulate the pressure in the reactor. After calcination and subsequent cooling down to the reaction temperature of 240 °C in Ar at atmospheric pressure (see Section 2.1), the pressure in the reactor was increased to the reaction pressure (5 bar) in a flow of the reaction gas mixture.

In the kinetic measurements, the freshly calcined catalyst sample was first exposed to a <sup>13</sup>CO<sub>2</sub>/H<sub>2</sub> mixture until a steady-state was reached (15% <sup>13</sup>CO<sub>2</sub>, 45% H<sub>2</sub>, balance Ar; 30 Nml min<sup>−1</sup>). This usually took approximately 100 minutes. Afterwards, different amounts of <sup>12</sup>CO (between 0.5 and 15%) were stepwise added to the <sup>13</sup>CO<sub>2</sub>/H<sub>2</sub> gas mixture by gradually replacing Ar while keeping the <sup>13</sup>CO<sub>2</sub>/H<sub>2</sub> ratio constant at 1/3 (15% <sup>13</sup>CO<sub>2</sub>/45% H<sub>2</sub>/0.5–15% <sup>12</sup>CO/balance Ar). Finally, the activity was measured once again in the presence of only <sup>13</sup>CO<sub>2</sub> in order to check for possible changes of the catalyst performance upon reaction in CO containing reaction atmospheres.

The influent and effluent gases were analyzed by mass spectrometry (Pfeiffer Vacuum HiQuad QMG 700). In all measurements masses 18, 28, 29, 31, 32, 44 and 45 were monitored. MeOH was identified *via* masses 31 and 32, which represent the strongest signals for MeOH containing <sup>12</sup>C and <sup>13</sup>C, respectively. Based on the molar flow rate of MeOH formed under differential reaction conditions ( $\dot{n}_{\text{MeOH,out}}/\text{CO}_2$  and CO conversions  $\leq 1\%$ ) and the absolute amount of Au metal ( $m_{\text{Au}}$ ), the Au mass-normalized MeOH formation rates ( $R_{\text{MeOH}}$ ) were calculated according to eqn (4). Turnover frequencies (TOFs) were calculated based on these Au mass-normalized reaction rates, the molar mass of Au ( $M_{\text{Au}}$ ), and

the Au dispersion ( $D_{\text{Au}}$ , obtained from TEM imaging) following eqn (5). Please note that these are normalized to the absolute amount of Au surface atoms rather than to the active site(s) for MeOH formation, which are not known for Au/ZnO catalysts so far. The selectivity for MeOH formation ( $S_{\text{MeOH}}$ ) is defined as the ratio of the MeOH formation rate to the overall CO<sub>2</sub> hydrogenation rate (to MeOH and CO, see eqn (6)).

$$R_{\text{MeOH}} = \frac{\dot{n}_{\text{MeOH,out}}}{m_{\text{Au}}} \quad (4)$$

$$\text{TOF}_{\text{MeOH}} = \frac{R_{\text{MeOH}} \times M_{\text{Au}}}{D_{\text{Au}}} \quad (5)$$

$$S_{\text{MeOH}} = \frac{R_{\text{MeOH}}}{R_{\text{CO}_2}} = \frac{R_{\text{MeOH}}}{R_{\text{MeOH}} + R_{\text{CO}}} \quad (6)$$

Calibration on an absolute scale was realized by comparison with the signal of a test gas containing a well-defined amount (partial pressure) of MeOH, and secondly by a direct comparison between GC and MS measurements under various reaction conditions (with different MeOH formation rates) during the CO<sub>2</sub> hydrogenation on Au/ZnO. Additionally, an isotopic exchange between <sup>13</sup>CO<sub>2</sub> and <sup>12</sup>CO was separately determined over the Au/ZnO catalyst under identical reaction conditions (same temperature, pressure and space velocity as during the reaction), and was found to be negligible under present reaction conditions.

## 3. Results and discussion

### 3.1. Catalyst characterization

The Au loading of the Au/ZnO catalyst was determined by inductively coupled plasma optical emission spectroscopy (ICP-OES) and amounts to 1.0 wt%. TEM images of the sample after O400 pretreatment revealed an even distribution of the Au nanoparticles on the ZnO support. A representative TEM image of the Au/ZnO catalyst after O400 pre-treatment as well as the corresponding Au particle size distribution, which is obtained from the evaluation of more than 400 Au particles, are shown in Fig. 1. From the Au particle size distribution the volume–area mean diameter of the Au particles was determined to be  $2.4 \pm 0.4$  nm, corresponding to a Au dispersion of 48.5%. The surface area of the Au/ZnO catalyst after calcination was  $42 \text{ m}^2 \text{ g}^{-1}$  (measured by low temperature N<sub>2</sub> adsorption). A summary of the physical properties of the freshly calcined Au/ZnO catalyst is given in Table 1.

Note that we demonstrated already in a previous study that the changes in the average Au particle size and size distribution as well as the surface area of the Au/ZnO catalyst during its exposure to reaction conditions are negligible.<sup>32</sup>

### 3.2. MeOH formation from <sup>13</sup>CO<sub>2</sub> and <sup>12</sup>CO

We will first focus on the overall MeOH formation rates during the CO and CO<sub>2</sub> hydrogenation in CO/H<sub>2</sub> and CO<sub>2</sub>/H<sub>2</sub> reaction gas mixtures, respectively, at 5 bar and 240 °C. For the CO<sub>2</sub>/H<sub>2</sub> reaction gas mixture we also additionally measured the influence of CO addition on the overall MeOH formation rate. Such data



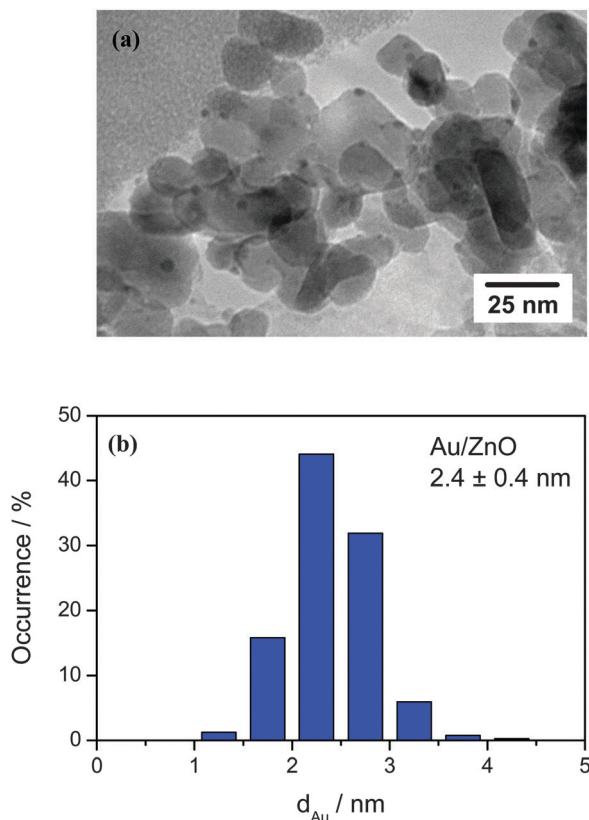


Fig. 1 (a) Representative TEM image of the Au/ZnO catalyst after calcination in 1% O<sub>2</sub>/Ar at 400 °C and at atmospheric pressure for 1 h (O400) and (b) the corresponding particle size distribution.

Table 1 Au particle size, dispersion and catalyst surface area of the Au/ZnO catalyst after calcination in 1% O<sub>2</sub>/Ar at 400 °C for 1 h (O400)

	After O400
Au particle size <sup>a</sup> /nm	2.4 ± 0.4
Dispersion <sup>b</sup> /%	48.5
Surface area <sup>c</sup> /m <sup>2</sup> g <sub>cat</sub> <sup>-1</sup>	41.6

<sup>a</sup> Measured by TEM. <sup>b</sup> Calculated assuming hemispherical Au nanoparticles. <sup>c</sup> Measured by low temperature N<sub>2</sub> adsorption (BET).

had been measured before, but only at a total pressure of 50 bar.<sup>32</sup> Time dependent turnover frequencies (TOFs) of MeOH formation during CO hydrogenation (15% CO, 45% H<sub>2</sub>, balance Ar) and CO<sub>2</sub> hydrogenation (15% CO<sub>2</sub>, 45% H<sub>2</sub>, balance Ar) on a freshly pre-treated Au/ZnO catalyst (O400) are presented in Fig. 2. Obviously, both the reaction characteristics and the MeOH formation rates differ significantly, despite the identical partial pressures of CO and CO<sub>2</sub> and, hence, identical C/H ratios. The initial activity (TOF) of Au/ZnO for the (overall) CO<sub>2</sub> hydrogenation is  $\sim 5 \times 10^{-3} \text{ s}^{-1}$ , and it then decreases steadily in an approximately exponential way, until reaching a final activity of  $3.4 \times 10^{-3} \text{ s}^{-1}$  after 1000 min on stream. Focusing on methanol formation only, the situation is very different. It starts at  $1.1 \times 10^{-3} \text{ s}^{-1}$  and increases during the initial 70 min to  $1.8 \times 10^{-3} \text{ s}^{-1}$ . Afterwards there is a slight decrease in activity with time on stream (deactivation), which finally results in a TOF of  $1.5 \times 10^{-3} \text{ s}^{-1}$  after 1000 min, and when

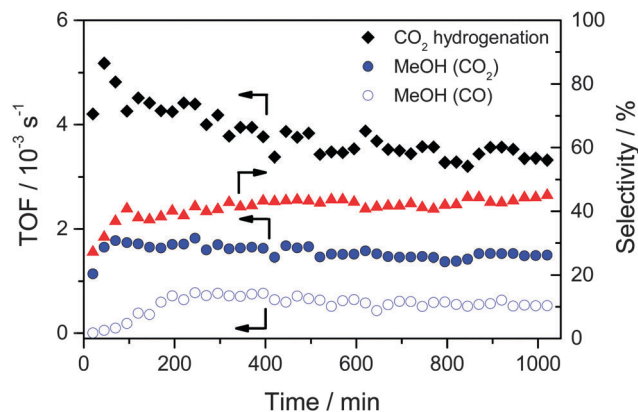


Fig. 2 Time dependent MeOH formation activity (TOF) of the Au/ZnO catalyst (STREM Chemicals) during CO<sub>2</sub> hydrogenation (●, 15% CO<sub>2</sub>/45% H<sub>2</sub>/balance Ar) and CO hydrogenation (○, 15% CO/45% H<sub>2</sub>/balance Ar) at 5 bar and 240 °C after calcination in 1% O<sub>2</sub>/Ar at 20 Nml min<sup>-1</sup> and 400 °C for 1 h (O400). For CO<sub>2</sub> hydrogenation the activity (TOF) (◆) and selectivity (▲) for MeOH formation are also included.

almost no more changes in activity are observed. The initial increase in the MeOH formation rate is also reflected by the selectivity towards MeOH formation, which increases over the first 100 min, from  $\sim 25$  to  $\sim 40\%$ . For the remaining time, the selectivity continues to increase slowly, to about 45% after 1000 min on stream. These results agree closely with previous findings under similar reaction conditions,<sup>32</sup> but differ somewhat from the reaction characteristics of Au/ZnO during CO<sub>2</sub> hydrogenation at 50 bar. For the latter case we recently reported that the catalyst is immediately in its most active state, and that there is hardly any deactivation with time on stream.<sup>32</sup>

Moving on to the CO hydrogenation, this situation changes significantly. Here the initial activity at 5 bar is close to zero and increases steadily during the reaction, until it reaches its maximum value after about 200 min (TOF  $0.8 \times 10^{-3} \text{ s}^{-1}$ ). Subsequently it decreases continuously with time on stream, reaching a steady-state activity of  $0.5 \times 10^{-3} \text{ s}^{-1}$  after 1000 min. The discrepancy between the initial activity for the CO<sub>2</sub> hydrogenation to methanol and the CO hydrogenation (to methanol) already indicated that under present reaction conditions methanol formation from CO<sub>2</sub> does not proceed *via* the formation of CO (by the RWGS reaction) and its subsequent hydrogenation to MeOH, as for the latter reaction the initial activity is close to zero. The present findings for CO hydrogenation at 5 bar and its temporal evolution also differ remarkably from the behavior at 50 bar under otherwise identical conditions.<sup>32</sup> In the latter case, we found that the activity is the highest right at the start of the reaction, followed by a continuous slight decrease with time on stream for at least 1000 min.

The difference in the initial phase of the reaction, where we observed an increase in the methanol formation rate for both CO<sub>2</sub> hydrogenation and CO hydrogenation for the reaction at 5 bar, while at 50 bar it was about constant, may well be due to an experimental artifact. While for the reaction at 5 bar the first gas sample was taken at about 25 min after changing from bypass to the reaction gas mixture, this delay time was much





longer for the reaction at 50 bar, since it took longer to reach steady-state conditions in the reactor gas composition. When the first gas sample was taken at 50 bar, the catalyst was exposed already for more than 1 h to a gas atmosphere which was getting increasingly closer to the final reaction gas composition. In that case it is not surprising that the initial activation observed at 5 bar is not detected for the reaction at 50 bar, but occurs before the first probe is taken. Finally we would like to note that the long term performance of the Au/ZnO catalyst, which is relevant for possible technical applications, is very promising. For the operation at 50 bar we did not find any indication for deactivation over 50 hours on stream.

The comparison of the MeOH formation activities from CO<sub>2</sub> and CO under steady-state reaction conditions shows that this is significantly lower, by a factor of about 3, during the CO hydrogenation ( $3.6 \times 10^{-6} \text{ mol s}^{-1} \text{ g}_{\text{Au}}^{-1}$  and  $1.2 \times 10^{-6} \text{ mol s}^{-1} \text{ g}_{\text{Au}}^{-1}$  for CO<sub>2</sub> hydrogenation and for CO hydrogenation, respectively, corresponding to TOFs of  $1.5 \times 10^{-3} \text{ s}^{-1}$  and  $0.5 \times 10^{-3} \text{ s}^{-1}$ ). This trend is consistent with previous results at 50 bar, demonstrating that at both 5 and 50 bar CO<sub>2</sub> hydrogenation on Au/ZnO is faster than CO hydrogenation at 240 °C under steady-state conditions.

Next we determined the influence of adding various amounts of CO (0.5–15% CO) to the CO<sub>2</sub>/H<sub>2</sub> reaction gas mixture on the

overall MeOH formation rate of Au/ZnO, the corresponding TOFs obtained under steady state conditions are shown in Fig. 3. Evidently, the addition of up to 15% CO has almost no effect on the MeOH formation rate under present reaction conditions. Similar to the reaction in a CO<sub>2</sub>/H<sub>2</sub> mixture, the Au mass-normalized MeOH formation rates in all different CO<sub>2</sub>/CO/H<sub>2</sub> mixtures are about  $3.6 \times 10^{-6} \text{ mol s}^{-1} \text{ g}_{\text{Au}}^{-1}$ , which corresponds to a TOF of  $1.5 \times 10^{-3} \text{ s}^{-1}$  (Table 2). These MeOH formation rates are also comparable to the value reported previously for the CO<sub>2</sub> hydrogenation on the same Au/ZnO catalyst under identical reaction conditions ( $3.8 \times 10^{-6} \text{ mol s}^{-1} \text{ g}_{\text{Au}}^{-1}$ ,  $1.6 \times 10^{-3} \text{ s}^{-1}$ ) at 5 bar and 240 °C.<sup>31</sup> Moreover, also the selectivity to MeOH in CO<sub>2</sub>/H<sub>2</sub> mixtures in both studies is almost identical (44% and 48%, respectively). Hence, in spite of the increasing total amount of carbon containing species (CO<sub>2</sub> and CO) and the increased C/H ratio, there is no significant increase in the rate of MeOH formation. This indicates that, similar to previous conclusions for the CO<sub>2</sub> hydrogenation reaction at 50 bar,<sup>32</sup> CO is not an intermediate in the CO<sub>2</sub> hydrogenation reaction (eqn (1)). If CO<sub>2</sub> is first converted to CO, *via* the RWGS reaction, and the resulting CO is subsequently hydrogenated to MeOH (eqn (2)), one would expect an increase in the MeOH formation rate with increasing CO content, independent of whether the first reaction step (RWGS of CO<sub>2</sub>) or the second step (CO hydrogenation) is rate limiting. This is obviously not the case under present reaction conditions. At 50 bar under otherwise identical reaction conditions, the MeOH formation rate even decreased as CO was added to a reaction gas mixture containing CO<sub>2</sub> only.<sup>32</sup> Hence, in both cases hydrogenation of CO<sub>2</sub> and CO seem to proceed *via* different reaction pathways, which can occur in parallel.

Further information on the effect of CO on the hydrogenation of CO<sub>2</sub> was obtained from isotope labelling experiments, determining <sup>12</sup>CH<sub>3</sub>OH and <sup>13</sup>CH<sub>3</sub>OH product formation from <sup>13</sup>CO<sub>2</sub>/<sup>12</sup>CO/H<sub>2</sub> mixtures. This provides direct information on the carbon source for MeOH. The individual contributions of <sup>13</sup>CO<sub>2</sub> and <sup>12</sup>CO to the total amount of MeOH formed at 5 bar and 240 °C with increasing amounts of <sup>12</sup>CO added to the <sup>13</sup>CO<sub>2</sub>/H<sub>2</sub>/Ar mixture are presented in Fig. 4a (see also Table 2). As already described above, the overall MeOH formation rate is essentially the same for all gas mixtures except for CO only. The activity for MeOH formation from CO<sub>2</sub>, however, slightly decreases upon the addition of 0.5% CO (CO<sub>2</sub>/CO = 30/1), from  $1.5 \times 10^{-3} \text{ s}^{-1}$  to  $1.2 \times 10^{-3} \text{ s}^{-1}$  (Fig. 4b). Obviously, MeOH

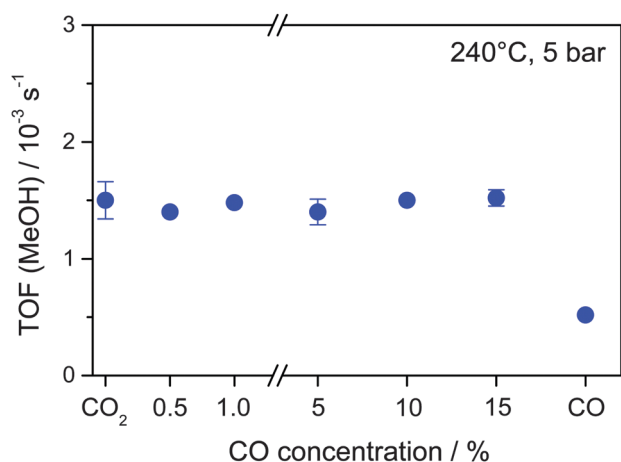


Fig. 3 Steady-state MeOH formation rates (TOFs) during <sup>13</sup>CO<sub>2</sub> hydrogenation (15% CO<sub>2</sub>, 45% H<sub>2</sub>, balance Ar) in the absence and presence of 0.5–15% <sup>12</sup>CO as well as during the <sup>12</sup>CO hydrogenation (15% CO, 45% H<sub>2</sub>, balance Ar) on a Au/ZnO catalyst (STREM Chemicals) at 5 bar and 240 °C.

Table 2 Au mass-normalized MeOH formation rates, turnover frequencies (TOFs) and MeOH isotopic compositions during <sup>13</sup>CO<sub>2</sub> hydrogenation (15% CO<sub>2</sub>, 45% H<sub>2</sub>) in the absence and presence of <sup>12</sup>CO (0.5–15%) in the reactant gas mixture as well as during pure <sup>12</sup>CO hydrogenation at 5 bar and 240 °C under steady-state conditions over a Au/ZnO catalyst (STREM Chemicals)

CO concentration/%	MeOH formation rate/ $10^{-6} \text{ mol s}^{-1} \text{ g}_{\text{Au}}^{-1}$	MeOH formation TOF/ $10^{-3} \text{ s}^{-1}$	Fraction of MeOH from <sup>13</sup> CO <sub>2</sub>	Fraction of MeOH from <sup>12</sup> CO
0	3.6	1.5	100	0
0.5	3.3	1.4	90	10
1	3.5	1.5	82	18
5	3.4	1.4	83	17
10	3.6	1.5	80	20
15	3.6	1.5	78	22
Pure CO	1.2	0.5	0	100



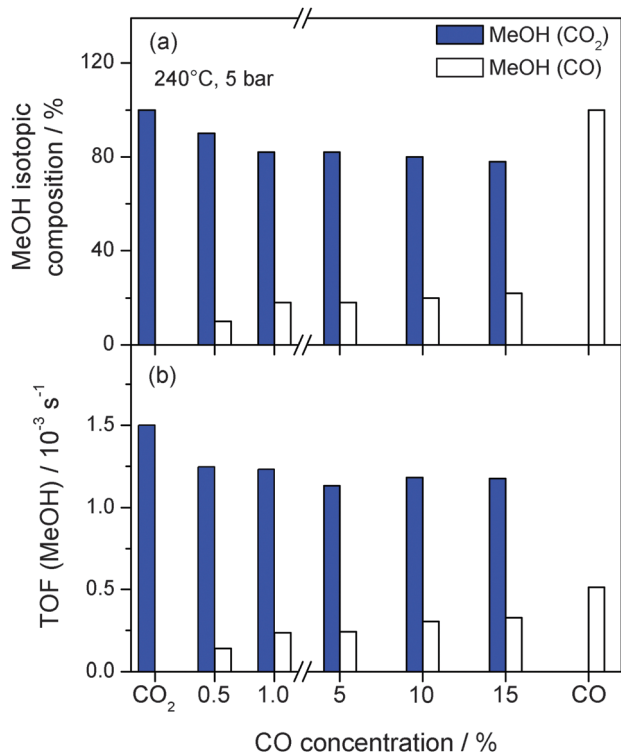


Fig. 4 (a) Ratios of MeOH formation from CO<sub>2</sub> and CO, respectively, during <sup>13</sup>CO<sub>2</sub> hydrogenation (15% CO<sub>2</sub>, 45% H<sub>2</sub>, balance Ar) in the absence and presence of 0.5–15% <sup>12</sup>CO as well as during the <sup>12</sup>CO hydrogenation (15% CO, 45% H<sub>2</sub>, balance Ar) and (b) the corresponding MeOH formation activities (TOFs) on a Au/ZnO catalyst (STREM Chemicals) at 5 bar and 240 °C.

formation from CO<sub>2</sub> is somewhat inhibited by the presence of CO. At the same time, about 10% of the overall MeOH formed originate from CO (TOF =  $0.14 \times 10^{-3} \text{ s}^{-1}$ ), although the partial pressure of CO is much lower than that of CO<sub>2</sub>. Accordingly, the fraction of MeOH from CO<sub>2</sub> decreases from 100% (for CO<sub>2</sub>/H<sub>2</sub> only) to 90% in the presence of 0.5% CO (Fig. 4a).

Upon increasing the CO concentration to 1% (CO<sub>2</sub>/CO = 15/1) the fraction of MeOH formed from CO<sub>2</sub> decreases further to approximately 80%. Hence, up to 1% CO in the reaction gas mixture there is an almost linear decrease/increase in the MeOH formation rate from CO<sub>2</sub>/CO, respectively. Increasing the CO concentration further to 5% and higher (up to 15%; CO<sub>2</sub>/CO = 1/1), however, does not result in significant changes in the CO<sub>2</sub> and CO contributions to the total MeOH production. For each of the reaction gas mixtures tested (15% CO<sub>2</sub>, 45% H<sub>2</sub>, +1%, +5%, +10%, and +15% CO, balance Ar), the fractions of MeOH from CO<sub>2</sub> and CO are about 80% and 20%, respectively, (see Table 2). Hence, even for identical partial pressures of CO and CO<sub>2</sub> the majority of MeOH formed originates from CO<sub>2</sub>, clearly indicating that over a wide range of CO<sub>2</sub>/CO compositions, CO<sub>2</sub> is the main carbon source in MeOH formation under present reaction conditions (240 °C, 5 bar). Moreover, there is no further increase in the MeOH formation rate from CO upon increasing the CO concentration to values higher than 1%. This can be most easily explained by a saturation of CO adsorption sites under these conditions, which results in a reaction order for CO close to zero

for CO concentrations of 1% and higher. Remarkably, there is also no further inhibition of the CO<sub>2</sub> hydrogenation upon CO addition, clearly demonstrating that the main reaction pathway for this reaction is not affected by the increasing presence of CO. This situation, however, is different for the other products formed (MeOH and water), which have been demonstrated to have an inhibiting effect on the MeOH formation rate on Au/ZnO (similar to Cu-based catalysts).<sup>32</sup> This is further evidence that the dominant reaction pathways of both reactions, CO<sub>2</sub> and CO hydrogenation, proceed parallel to and are independent of each other. This finding agrees well with our previous findings, where we came to similar conclusions regarding the influence of CO on the overall MeOH formation rate for the reaction at 50 bar.<sup>32</sup> In that study we had also performed spectroscopic measurements in order to detect differences in the reaction mechanism, *e.g.*, different adsorption sites for CO and CO<sub>2</sub>, following the formation of adsorbed surface species during CO<sub>2</sub> hydrogenation and CO hydrogenation under reaction conditions (240 °C, 5 bar) by diffuse reflectance infrared Fourier transform spectroscopy (DRIFTS).<sup>32</sup> From these measurements it was, however, not possible to derive any insights on the adsorption sites for CO or CO<sub>2</sub>.

It should be noted that although independent of the CO<sub>2</sub>/CO ratio the majority of MeOH results from CO<sub>2</sub> hydrogenation, this does not mean that MeOH formation from CO is little effective. This is illustrated best by the fact that even at a composition of CO<sub>2</sub>/CO = 15/0.5, about 10% of the resulting MeOH comes from CO hydrogenation, which is significantly more than expected from the composition of the reaction gas (assuming reaction orders of 1 for CO<sub>2</sub> and CO). On the other hand, considering the overall objective of our work to efficiently convert CO<sub>2</sub> to methanol, it is most important whether the formation of CO does reduce the activity for CO<sub>2</sub> hydrogenation to methanol in general, which is hardly the case.

In this sequence of measurements we had not considered so far that the addition of CO to the CO<sub>2</sub>/H<sub>2</sub> mixture at constant CO<sub>2</sub> and H<sub>2</sub> partial pressures results in increasingly higher C/H ratios than during the initial CO<sub>2</sub> hydrogenation (CO<sub>2</sub>/H<sub>2</sub> = 1/3). Since this may hamper the understanding of the effect of CO on the hydrogenation of CO<sub>2</sub>, we also tested the reaction at a similar C/H ratio of 1/3 (with 45% H<sub>2</sub>), using a reaction gas mixture of 7.5% <sup>13</sup>CO<sub>2</sub>/7.5% <sup>12</sup>CO/45% H<sub>2</sub> (balance Ar). Comparable with the reaction in the presence of 15% CO<sub>2</sub> and 15% CO, this again results in an equimolar CO<sub>2</sub>/CO ratio, but this time with a C/H ratio of 1/3, identical to the original gas mixture during CO<sub>2</sub> hydrogenation only (15% CO<sub>2</sub>, 45% H<sub>2</sub>). In that case the overall MeOH formation rate is slightly lower compared to the carbon rich reaction atmosphere (TOF  $1.1 \times 10^{-3} \text{ s}^{-1}$ ), but the fractions of MeOH formed from CO<sub>2</sub> and CO (77% and 23%, respectively) are almost identical to the reaction atmosphere with 15% CO<sub>2</sub> and 15% CO. Obviously, the ratio of MeOH formed from CO<sub>2</sub> and CO does not depend on the C/H ratio under present reaction conditions. This also means that the direct comparison between CO<sub>2</sub>/H<sub>2</sub> and CO<sub>2</sub>/CO/H<sub>2</sub> is possible despite the increasing amount of carbon in the reaction gas feed.

In another additional measurement we also tested for changes in the MeOH formation rate upon increasing the partial pressure of



CO<sub>2</sub>, while keeping the partial pressure of H<sub>2</sub> constant. Hence, instead of adding CO we added CO<sub>2</sub> to the original reaction gas mixture, which equally results in an increased C/H ratio, similar to the above described experiments (CO<sub>2</sub> + CO). The corresponding results are shown in the ESI† (Fig. S1). In this case there is almost no change in the MeOH formation rate, which stays almost constant at about  $3.8 \times 10^{-6} \text{ mol s}^{-1} \text{ g}_{\text{Au}}^{-1}$ . Moreover, there are also no significant changes in the selectivity for MeOH formation, which is in between 44% and 41% for all reaction gas mixtures investigated (15–30% CO<sub>2</sub>, 45% H<sub>2</sub>, balance Ar). Hence, similar to the above described findings for CO, all CO<sub>2</sub> adsorption sites seem to be blocked in a reaction gas mixture containing 15% CO<sub>2</sub>, and further addition of CO<sub>2</sub> is not beneficial for the MeOH formation rate (zero reaction order for CO<sub>2</sub>). However, considering the lower MeOH formation rates in the presence of 7.5% CO<sub>2</sub> as described above (7.5% CO<sub>2</sub>, 7.5% CO, 45% H<sub>2</sub>) one can assume that for the CO<sub>2</sub> content lower than 15% CO<sub>2</sub> this is not true any longer, and the reaction order for CO<sub>2</sub> becomes positive at lower CO<sub>2</sub> partial pressures.

Regarding the main source of carbon in the MeOH formation on supported Au catalysts, our findings are also in agreement with an earlier proposal from Sakurai *et al.*, who also claimed that MeOH is mainly formed *via* the CO<sub>2</sub> hydrogenation.<sup>53</sup> This conclusion was based on a comparison of the CO<sub>2</sub> hydrogenation and CO hydrogenation activities over Au catalysts and, hence, neither in the presence of both reactants simultaneously nor directly by isotope labelling experiments. On the other hand, the results obtained for the Au/ZnO catalyst in this work are similar to the results of previous tracer atom experiments on Cu-based catalysts. First experiments to determine the main source of carbon in MeOH formation from CO<sub>2</sub>/CO/H<sub>2</sub> mixtures on a commercial copper-containing oxide catalyst and on a Cu/ZnO/Al<sub>2</sub>O<sub>3</sub> catalyst were reported by Rozovskii *et al.* and Chinchén *et al.*, respectively, using <sup>14</sup>C-labelled species.<sup>48,51</sup> Under conditions similar to those employed industrially, *i.e.*, at 50 bar and temperatures between 180 and 250 °C, both studies arrived at the conclusion that MeOH was predominantly formed from CO<sub>2</sub>, using reaction mixtures containing 20% CO<sub>2</sub>/1% CO<sup>51</sup> or 10% CO<sub>2</sub>/10% CO.<sup>48</sup> Chinchén *et al.* additionally also varied the ratio of the partial pressures of CO<sub>2</sub> and CO. In that case they found that at higher partial pressures of CO<sub>2</sub> (CO<sub>2</sub>:CO = 1:2) MeOH was essentially formed from CO<sub>2</sub> only, and that MeOH formation from CO occurred only at extremely low levels of CO<sub>2</sub> (<100 ppm CO<sub>2</sub>).<sup>48</sup> In another more recent isotope labelling experiment on Cu-based catalysts performed at 30 bar and 230 °C with a gas mixture containing 8% <sup>13</sup>CO<sub>2</sub>/6% CO/59% H<sub>2</sub> (balance inert gas), Studt *et al.* found that more than 90% of the resulting MeOH originated from CO<sub>2</sub>, both for Cu supported on irreducible MgO, which exhibited a poor MeOH formation rate, and also for Cu on ZnO, which exhibits a high turnover MeOH rate.<sup>45</sup> Although the reaction conditions in these studies were markedly different from ours, in particular the total pressure during the reaction, there is nevertheless good agreement on the dominant contribution of CO<sub>2</sub> hydrogenation to MeOH, which points to rather similar reaction characteristics on supported Cu and Au catalysts. Similar findings, yet for much lower

total pressures, were reported by Yang *et al.*,<sup>52</sup> who observed for the reaction of a <sup>12</sup>CO<sub>2</sub>/<sup>13</sup>CO/D<sub>2</sub> reaction gas mixture (1:1:6) on a Cu/SiO<sub>2</sub> catalyst under almost identical reaction conditions (6 bar and 240 °C), that also at much lower pressures than in the studies cited above the majority (78%) of MeOH formed originates from CO<sub>2</sub>.

### 3.3. Influence of the reaction temperature on MeOH formation from CO<sub>2</sub>

For the reaction gas mixture with 15% <sup>13</sup>CO<sub>2</sub>/15% CO/45% H<sub>2</sub>, we also investigated changes in the isotopic composition of the product MeOH with increasing reaction temperatures at a constant total pressure of 5 bar. After reaching a steady-state situation at 240 °C, the reaction temperature was increased to 270 °C and finally to 300 °C. The corresponding MeOH formation rates and the isotopic composition of MeOH are plotted in Fig. 5 (see also Table 3 and Table S3, ESI†). As expected for the kinetically controlled regime (note that both CO<sub>2</sub> and CO conversion were always well below the thermodynamic limit), the overall rate of MeOH formation increases with increasing reaction temperature, from  $3.6 \times 10^{-6} \text{ mol s}^{-1} \text{ g}_{\text{Au}}^{-1}$  (TOF  $1.5 \times 10^{-3} \text{ s}^{-1}$ ) to  $8.6 \times 10^{-6} \text{ mol s}^{-1} \text{ g}_{\text{Au}}^{-1}$  ( $3.6 \times 10^{-3} \text{ s}^{-1}$ ) and finally to  $10.4 \times 10^{-6} \text{ mol s}^{-1} \text{ g}_{\text{Au}}^{-1}$  ( $4.4 \times 10^{-3} \text{ s}^{-1}$ ) at 240 °C, 270 °C, and 300 °C, respectively. Although the MeOH formation rate from CO<sub>2</sub> hydrogenation also increases with increasing temperature, its fraction of the overall MeOH formation decreases

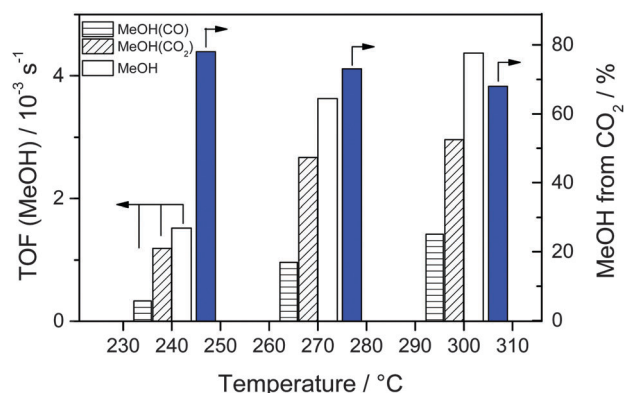


Fig. 5 MeOH formation rates (TOFs, left axis) and the fraction of MeOH formed from <sup>13</sup>CO<sub>2</sub> (right axis) under steady-state conditions during reaction in 15% <sup>13</sup>CO<sub>2</sub>/15% <sup>12</sup>CO/45% H<sub>2</sub> (CO<sub>2</sub>/CO = 1/1) at 5 bar on a Au/ZnO catalyst (STREM Chemicals) at various temperatures between 240 and 300 °C.

Table 3 Au mass-normalized MeOH formation rates, turnover frequencies (TOFs), and fraction of MeOH formation from <sup>13</sup>CO<sub>2</sub> during hydrogenation of a gas mixture containing 15% <sup>13</sup>CO<sub>2</sub>/15% <sup>12</sup>CO/45% H<sub>2</sub> (balance Ar) at 5 bar under steady-state conditions over a Au/ZnO catalyst (STREM Chemicals) at different temperatures between 240 and 300 °C

Temperature/ °C	MeOH formation rate/ $10^{-6} \text{ mol s}^{-1} \text{ g}_{\text{Au}}^{-1}$	MeOH TOF/ $10^{-3} \text{ s}^{-1}$	Fraction of MeOH from <sup>13</sup> CO <sub>2</sub>
240	3.6	1.5	78
270	8.6	3.6	73
300	10.4	4.4	68



due to the more pronounced increase of the CO hydrogenation with temperature, from about 78% at 240 °C *via* 73% at 270 °C to finally 68% at 300 °C. Obviously, the temperature has a pronounced influence on the ratio of the (parallel) reaction pathways for CO<sub>2</sub> and CO hydrogenation, with continuously less contribution from CO<sub>2</sub> with increasing temperatures. Such tendency had already been reported by Sakurai *et al.*<sup>53</sup> when comparing the CO<sub>2</sub> and CO hydrogenation activities of Au/ZnO catalysts at temperatures between 150 and 400 °C and at 8 bar total pressure. They observed that up to 250 °C the MeOH yield from CO<sub>2</sub> (for CO<sub>2</sub>/H<sub>2</sub> = 3 and for CO<sub>2</sub>/H<sub>2</sub> = 2) was higher than that from CO (CO/H<sub>2</sub> = 2). At higher temperatures ( $\geq 300$  °C), however, the MeOH yield from the CO/H<sub>2</sub> reaction gas mixture became dominant. While their findings are in good agreement with our present results, both with the reaction activities measured separately in CO<sub>2</sub>/H<sub>2</sub> and CO/H<sub>2</sub> gas mixtures at 240 °C, and with the temperature dependent trend in the activities for CO<sub>x</sub> hydrogenation in the CO<sub>2</sub>/CO/H<sub>2</sub> mixture described above, their proposal was somewhat tentative since those authors did not perform measurements in the simultaneous presence of both CO and CO<sub>2</sub>.

In a recent study on MeOH formation on the Au/ZnO catalyst at pressures between 20 and 40 bar and at a temperature of 300 °C, Strunk *et al.* compared the activity of the catalyst for MeOH formation in CO<sub>2</sub>-containing and CO<sub>2</sub>-free reaction gas mixtures (CO/H<sub>2</sub>).<sup>54</sup> They found that the partial replacement of CO by CO<sub>2</sub> at 300 °C (switching from 15% CO/85% H<sub>2</sub> to 6% CO/8% CO<sub>2</sub>/64% H<sub>2</sub>) resulted in lower MeOH formation rates.<sup>54</sup> (Note that this involved also a change in the C/H ratio.) They explained this decrease of the MeOH formation rate in the presence of CO<sub>2</sub> by either blocking oxygen vacancies on ZnO, which they had proposed as active sites for CO hydrogenation, by stable adsorbed formate species, or by the annihilation of these sites by the extra oxygen present in CO<sub>2</sub>. At first glance the higher MeOH formation rate in CO/H<sub>2</sub> compared to that in a CO<sub>2</sub>-containing reaction gas mixture (CO/CO<sub>2</sub>/H<sub>2</sub>) reported in their study seems to be in contrast to our previous findings at 50 bar and 240 °C on Au/ZnO, where (i) the addition of 5–15% CO to a 15% CO<sub>2</sub>/45% H<sub>2</sub> mixture resulted in a decrease in the MeOH formation rate and (ii) the MeOH formation rates in the presence of CO<sub>2</sub> (in the absence and presence of CO) were always significantly higher than those obtained in a reaction gas mixture containing only CO/H<sub>2</sub>.<sup>32</sup> However, taking into account the continuously higher contributions from CO to the overall MeOH formation with increasing temperatures, this apparent discrepancy can easily be rationalized. Obviously, CO hydrogenation becomes increasingly more important for MeOH formation upon increasing the reaction temperature from 240 to 300 °C.

The more pronounced increase in the MeOH formation from CO with increasing temperatures points directly to a higher apparent activation energy for the CO hydrogenation as compared to the CO<sub>2</sub> hydrogenation. To derive more insights into the apparent activation barriers in the MeOH formation *via* the CO<sub>2</sub> hydrogenation and the CO hydrogenation, we measured their activities in a temperature range between 220 °C

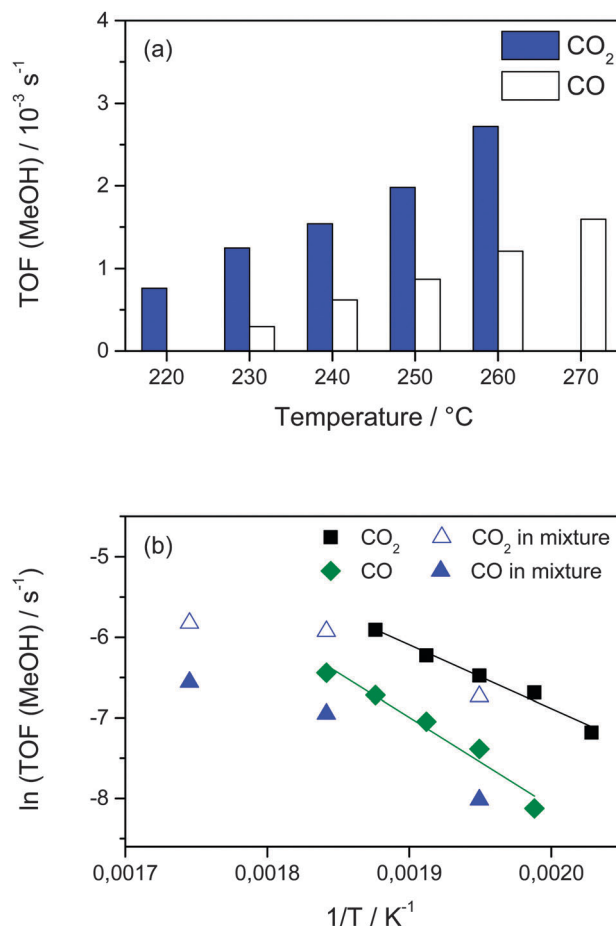


Fig. 6 (a) Steady-state MeOH formation rates (TOFs) during CO<sub>2</sub> (15% CO<sub>2</sub>, 45% H<sub>2</sub>, balance Ar) and CO (15% CO, 45% H<sub>2</sub>, balance Ar) hydrogenation at 5 bar and temperatures between 220 and 270 °C and (b) Arrhenius plots of the MeOH formation rates obtained in the above measurements. For comparison we also show the activities for MeOH formation from CO<sub>2</sub> and CO in a mixture containing 15% CO<sub>2</sub>, 15% CO, 45% H<sub>2</sub>, balance Ar.

and 270 °C in the CO<sub>2</sub>/H<sub>2</sub> and CO/H<sub>2</sub> mixtures. The results obtained are presented in Fig. 6a. They show that for both reactions the TOF for MeOH formation continuously increases as temperature increases. Consistent with the results presented above, the MeOH formation from CO<sub>2</sub> is always higher than that from CO in the temperature range investigated (up to 270 °C). The apparent activation energies for MeOH formation calculated from the temperature dependence of the rates are  $66 \pm 5$  and  $92 \pm 5$  kJ mol<sup>-1</sup> for the CO<sub>2</sub> hydrogenation and CO hydrogenation on Au/ZnO at 5 bar, respectively, (see Fig. 6b). For comparison, the activities for MeOH formation from CO<sub>2</sub> and CO measured in the simultaneous presence of CO and CO<sub>2</sub> (15% CO<sub>2</sub>/15% CO/45% H<sub>2</sub>) at 240 °C, 270 °C, and 300 °C are also included in this figure. For 240 °C and 270 °C the MeOH formation rates from CO<sub>2</sub> in the CO<sub>2</sub>/CO mixture and in pure CO<sub>2</sub> are rather close to each other and show an almost identical temperature dependency. Only at 300 °C the MeOH formation from CO<sub>2</sub> is somewhat lower than expected, but this may easily be rationalized by a decreasing selectivity for MeOH formation





with increasing reaction temperature.<sup>32</sup> Similar to that, also for MeOH formation from CO the activities are slightly higher for CO only than obtained in the presence of CO<sub>2</sub>, and the temperature dependence up to 270 °C seems comparable. Overall it is obvious from these measurements that the apparent activation energy for CO hydrogenation is higher compared to that for MeOH formation from CO<sub>2</sub>, for the individual reactions as well as for reaction gas mixtures containing CO<sub>2</sub> and CO. This provides additional evidence that the CO<sub>2</sub> hydrogenation to MeOH proceeds not *via* the RWGS reaction (eqn (1), see above). Otherwise, CO hydrogenation would be part of the MeOH formation from CO<sub>2</sub>, which accordingly should have at least the same activation barrier as CO hydrogenation. Hence, these results also indicate that CO<sub>2</sub> is directly hydrogenated to MeOH under present reaction conditions. Since neither for the CO<sub>2</sub> hydrogenation nor for the CO hydrogenation the nature and number of active sites or the local coverages of adspecies and reaction intermediates are known, the physical origin of different apparent activation energies and, hence, the increasing contribution from CO to the overall MeOH formation with increasing temperatures needs to be addressed in future studies.

In our previous studies we already compared Au catalysts with different oxide supports and different Au particle sizes (for Au/ZnO) in order to unravel the active site(s). Moreover, we also performed *operando* IR spectroscopic measurements during both CO<sub>2</sub> hydrogenation and CO hydrogenation on Au/ZnO to gain further insight into the nature of the adspecies formed during the reaction. So far, however, these measurements did not allow us to draw firm conclusions on the nature of the active site or the reaction intermediates. This is the topic of ongoing studies in our laboratory, which aim at gaining more mechanistic insight, for example, by using Au/ZnO catalysts with different Au loadings.

### 3.4. Consequences of our results on application in renewable energy storage

The main aim of the present study was to further elucidate the role of CO in the hydrogenation of CO<sub>2</sub> to MeOH. The latter reaction may be part of concepts for renewable energy storage, if the H<sub>2</sub> required for this reaction is produced by renewable energies. It may help to overcome natural fluctuations in the supply of renewable energy as well as to diminish the overall CO<sub>2</sub> emission. This, however, is only feasible if (i) the catalysts used for CO<sub>2</sub> hydrogenation are highly selective towards MeOH formation, (ii) the CO formed *via* the parallel RWGS reaction has no or only little detrimental effect on the MeOH formation activity from CO<sub>2</sub>, and (iii) the CO resulting from the RWGS reaction can also be efficiently hydrogenated to MeOH. We have already demonstrated previously that Au/ZnO catalysts, to the best of our knowledge, have higher selectivities towards MeOH formation in this process in comparison to commercial Cu-based systems.<sup>32</sup> Although there are also catalysts with even higher selectivities (up to 100%) under comparable reaction conditions,<sup>34–38</sup> during CO<sub>2</sub> hydrogenation on Au/ZnO there is always some CO present in the reaction gas atmosphere, whose partial pressure within the catalyst bed will increase together

with the formation of MeOH. The present study provided clear evidence that the presence of up to 15% CO in the reaction atmosphere has almost no influence on the overall MeOH formation under present reaction conditions (5 bar, 240 °C). Although MeOH formation from CO<sub>2</sub> is slightly diminished in the presence of CO, this is counterbalanced by additional MeOH formation from CO hydrogenation. The origin of the resulting MeOH formation, CO<sub>2</sub> or CO hydrogenation, was unraveled. It should be noted that different from the present findings for reaction at 5 bar the MeOH formation from CO<sub>2</sub> was found to decrease slightly in the presence of CO concentrations > 1% for reaction at 50 bar.<sup>32</sup> This has to be considered for practical applications, where the reaction will most likely be performed at rather high reaction pressures, due to higher MeOH yields at higher pressure.

After the principal potential of Au/ZnO catalysts for CO<sub>2</sub> hydrogenation to methanol has been clearly demonstrated, future work shall focus on (i) improving the activity and thus lower the catalyst costs and (ii) addressing mechanistic aspects by using *operando* spectroscopy. In this context the specific role of Au/ZnO is of particular interest.

## 4. Conclusions

From detailed kinetic isotope labelling measurements on MeOH formation from CO<sub>2</sub> in CO containing syngas mixtures (<sup>13</sup>CO<sub>2</sub>/CO/H<sub>2</sub>) on highly selective Au/ZnO catalysts, performed at 5 bar total pressure and in the temperature range of 240–300 °C, we arrived at the following conclusions:

1. Under present reaction conditions the activity of the Au/ZnO catalyst for CO<sub>2</sub> hydrogenation in CO<sub>2</sub>/H<sub>2</sub> is significantly higher than that for CO hydrogenation in CO/H<sub>2</sub> syngas. Moreover, for the reaction in CO<sub>2</sub>/CO/H<sub>2</sub> mixtures, up to equimolar amounts of CO and CO<sub>2</sub> (15% CO<sub>2</sub> and 15% CO), CO<sub>2</sub> is the preferred carbon source of MeOH.
2. During the reaction in CO<sub>2</sub>/CO/H<sub>2</sub> mixtures the fraction of MeOH formed from CO increases linearly from 10% to approximately 20% for the CO content up to 1%. At higher CO content, however, the changes in the CO contribution to the final MeOH product are negligible. This is tentatively explained by saturation of the active CO adsorption sites under these conditions.
3. The presence of CO in the reaction gas mixture has little effect on the activity of the Au/ZnO catalyst for CO<sub>2</sub> hydrogenation to MeOH, as indicated by the very small decay in the TOF for MeOH formation from CO<sub>2</sub>. Furthermore, the addition of CO (0.5–15% CO) to a gas mixture containing only CO<sub>2</sub>/H<sub>2</sub> has almost no effect on the overall MeOH formation rate of Au/ZnO.
4. From the fact that the main reaction pathway for CO<sub>2</sub> hydrogenation is little affected by the presence of CO we conclude that CO<sub>2</sub> and CO hydrogenation reactions proceed in parallel reaction pathways, independent of each other. Further evidence for this suggestion comes from (i) the time dependence of the reaction rates in CO<sub>2</sub>/H<sub>2</sub> and CO/H<sub>2</sub>, where the very low activity observed for CO hydrogenation in the initial phase of the reaction is in contrast to the much higher initial activity for methanol formation from CO<sub>2</sub> hydrogenation



and (ii) the significantly higher apparent activation energy of Au/ZnO for MeOH formation from CO compared to CO<sub>2</sub>.

5. The relative activities for CO and CO<sub>2</sub> hydrogenation depend strongly on the temperature. For reaction with equimolar amounts of CO<sub>2</sub> and CO the main carbon source for MeOH at reaction temperatures between 240 °C and 300 °C is always CO<sub>2</sub>, but with an increasing tendency towards CO hydrogenation with increasing temperatures. Hence, at even higher temperatures, CO is expected to eventually dominate the MeOH formation under otherwise identical conditions.

Considering (i) the similar trends when comparing the activities of CO hydrogenation and CO<sub>2</sub> hydrogenation as well as (ii) the qualitatively identical influence of CO addition to a CO<sub>2</sub>/H<sub>2</sub> gas mixture on the overall MeOH formation rate at 5 bar and at 50 bar, we are confident that the present findings are valid also at elevated pressures (at 50 bar), which are more relevant for practical applications. Overall, the results further underline the remarkable potential of Au/ZnO catalysts for application in the hydrogenation of CO<sub>2</sub> to “green MeOH” as an energy storage molecule.

## Acknowledgements

We gratefully acknowledge extended discussions with S. Dahl (Haldor Topsøe A/S).

## References

- 1 R. Schlögl, *Angew. Chem., Int. Ed.*, 2011, **50**, 6424.
- 2 R. Schlögl, *Nachr. Chem.*, 2012, **60**, 1.
- 3 G. A. Olah, *Angew. Chem., Int. Ed.*, 2004, **44**, 2636.
- 4 G. A. Olah, *Angew. Chem., Int. Ed.*, 2013, **52**, 104.
- 5 *Methanol: The Basic Chemical and Energy Feedstock of the Future*, ed. M. Bertau, H. Offermanns, L. Plass, F. Schmidt and H.-J. Wernicke, Springer Verlag, Heidelberg, 2013.
- 6 J. B. Hansen and P. E. Højlund Nielsen, *Handbook of Heterogeneous Catalysis*, Wiley VCH, 2008, vol. 13.13, p. 2920.
- 7 X. Xu and J. A. Moulijn, *Energy Fuels*, 1996, **10**, 305.
- 8 H. Yang, Z. Xu, M. Fan, R. Gupta, R. B. Slimane, A. E. Bland and I. Wright, *J. Environ. Sci.*, 2008, **20**, 14.
- 9 A. J. Hunt, E. H. K. Sin, R. Marriott and J. H. Clark, *ChemSusChem*, 2010, **3**, 306.
- 10 G. Ferey, C. Serre, T. Devic, G. Maurin, H. Jobic, P. L. Llewellyn, G. De Weireld, A. Vimont, M. Daturi and J. S. Chang, *Chem. Soc. Rev.*, 2011, **40**, 550.
- 11 W. Wang, S. Wang, X. Ma and J. Gong, *Chem. Soc. Rev.*, 2011, **40**, 3703.
- 12 M. Aresta, in *Activation of Small Molecules*, ed. W. B. Tolman, 2006, vol. 1, p. 1.
- 13 G. A. Olah, A. Goeppert and G. K. Surya Prakash, *J. Org. Chem.*, 2009, **74**, 487.
- 14 G. A. Olah, G. S. Prakash and A. Goeppert, *J. Am. Chem. Soc.*, 2011, **133**, 12881.
- 15 M. Behrens, F. Studt, I. Kasatkin, S. Köhl, M. Hävecker, F. Abild-Pedersen, S. Zander, F. Girgsdies, P. Kurr, B.-L. Knief, M. Tovar, R. W. Fischer, J. K. Nørskov and R. Schlögl, *Science*, 2012, **336**, 893.
- 16 M. Behrens, *Angew. Chem., Int. Ed.*, 2014, **53**, 12022.
- 17 A. Goeppert, M. Czaun, J. P. Jones, G. S. Prakash and G. A. Olah, *Chem. Soc. Rev.*, 2014, **43**, 7995.
- 18 The George Olah Renewable Methanol Plant, 2009, www.carbonrecycling.is.
- 19 H. H. Kung, *Catal. Rev.: Sci. Eng.*, 1980, **22**, 235.
- 20 K. Klier, *Adv. Catal.*, 1982, **31**, 243.
- 21 G. Ghiotti and F. Boccuzzi, *Catal. Rev.: Sci. Eng.*, 1987, **29**, 151.
- 22 J. C. J. Bart and R. P. A. Sneed, *Catal. Today*, 1987, **2**, 1.
- 23 G. C. Chinen, P. J. Denny, J. R. Jennings, M. S. Spencer and K. C. Waugh, *Appl. Catal.*, 1988, **36**, 1.
- 24 A. Kiennemann and J. P. Hindermann, *Stud. Surf. Sci. Catal.*, 1988, **35**, 181.
- 25 R. G. Herman, *Stud. Surf. Sci. Catal.*, 1991, **64**, 265.
- 26 K. C. Waugh, *Catal. Today*, 1992, **15**, 51.
- 27 X.-M. Liu, G. Q. Lu, Z.-F. Yan and J. Beltramini, *Ind. Eng. Chem. Res.*, 2003, **42**, 6518.
- 28 K. C. Waugh, *Catal. Lett.*, 2012, **142**, 1153.
- 29 L. C. Grabow and M. Mavrikakis, *ACS Catal.*, 2011, **1**, 365.
- 30 J. Graciani, K. Mudiyanse, F. Xu, A. E. Baber, J. Evans, S. D. Senanayake, D. J. Stacchiola, P. Liu, J. Hrbek and J. F. Sanz, *Science*, 2014, **345**, 546.
- 31 Y. Hartadi, D. Widmann and R. J. Behm, *ChemSusChem*, 2015, **8**, 456.
- 32 Y. Hartadi, D. Widmann and R. J. Behm, *J. Catal.*, 2015, **333**, 238.
- 33 E. L. Kunkes, F. Studt, R. Schlögl, F. Abild-Pedersen and M. Behrens, *J. Catal.*, 2015, **328**, 43.
- 34 J. Toyir, P. R. de la Piscina, J. L. G. Fierro and N. Homs, *Appl. Catal., B*, 2001, **29**, 207.
- 35 J. Sloczynski, R. Grabowski, A. Kozłowska, P. Olszewski, J. Stoch, J. Skrzypek and M. Lachowska, *Appl. Catal., A*, 2004, **278**, 11.
- 36 O. Martin, C. Mondelli, D. Curulla-Ferré, C. Drouilly, R. Hauert and J. Perez-Ramirez, *ACS Catal.*, 2015, **5**, 5607.
- 37 X.-L. Liang, X. Dong, G.-D. Lin and H.-B. Zhang, *Appl. Catal., B*, 2009, **88**, 315.
- 38 L. Jia, J. Gao, W. Fang and Q. Li, *Catal. Commun.*, 2009, **10**, 2000.
- 39 Z. S. Hong, Y. Cao, J. F. Deng and K. N. Fan, *Catal. Lett.*, 2002, **82**, 37.
- 40 R. Raudaskoski, M. V. Niemelä and R. L. Keiski, *Top. Catal.*, 2007, **45**, 57.
- 41 P. Gao, L. Zhong, L. Zhang, H. Wang, N. Zhao, W. Wei and Y. Sun, *Catal. Sci. Technol.*, 2015, **5**, 4365.
- 42 Z. Q. Wang, Z. N. Xu, S. Y. Peng, M. J. Zhang, G. Lu, Q. S. Chen, Y. Chen and G. C. Guo, *ACS Catal.*, 2015, **5**, 4255.
- 43 N. Y. Topsøe and H. Topsøe, *Top. Catal.*, 1999, **8**, 267.
- 44 S. Kuld, C. Conradsen, P. G. Moses, I. Chorkendorff and J. Sehested, *Angew. Chem., Int. Ed.*, 2014, **53**, 5941.
- 45 F. Studt, M. Behrens, E. L. Kunkes, N. Thomas, S. Zander, A. Tarasov, J. Schumann, E. Frei, J. B. Varley, F. Abild-Pedersen, J. K. Nørskov and R. Schlögl, *ChemCatChem*, 2015, **7**, 1105.



- 46 A. Le Valant, C. Comminges, C. Tisseraud, C. Canaff, L. Pinard and Y. Pouilloux, *J. Catal.*, 2015, **324**, 41.
- 47 C. Tisseraud, C. Comminges, T. Belin, H. Ahouari, A. Soualah, Y. Pouilloux and A. Le Valant, *J. Catal.*, 2015, **330**, 533.
- 48 G. C. Chinchin, M. S. Spencer, K. C. Waugh and D. A. Whan, *J. Chem. Soc., Faraday Trans. 1*, 1987, **83**, 2193.
- 49 M. Muhler, E. Törnqvist, L. P. Nielsen, B. S. Clausen and H. Topsøe, *Catal. Lett.*, 1994, **25**, 1.
- 50 G. Liu, D. Willcox, M. Garland and H. H. Kung, *J. Catal.*, 1985, **96**, 251.
- 51 A. Y. Rozovskii, *Russ. Chem. Rev.*, 1989, **58**, 41.
- 52 Y. Yang, C. A. Mims, D. H. Mei, C. H. F. Peden and C. T. Campbell, *J. Catal.*, 2013, **298**, 10.
- 53 H. Sakurai, S. Tsubota and M. Haruta, *Appl. Catal., A*, 1993, **102**, 125.
- 54 J. Strunk, K. Kähler, X. Xia, M. Comotti, F. Schüth, T. Reinecke and M. Muhler, *Appl. Catal., A*, 2009, **359**, 121.

